Substituent and Solvent Effects in the Insertion and Isomerization of Olefins by Platinum(bis-phosphine) Complexes: An ab Initio Study of the $Pt(PR_3)_2H(propene)^+$ Model Systems

Steven Creve,[†] Henk Oevering,[‡] and Betty B. Coussens*,[‡]

Department of Chemistry, University of Leuven, Celestijnenlaan 200F, B-3001 Heverlee, Belgium, and DSM Research, P.O. Box 18, 6160 MD Geleen, The Netherlands

Received August 12, 1998

Traditional ab initio (HF, MP2) and density functional theory (DFT) calculations are applied on the cationic $Pt(PR_3)_2(H)(propene)^+$ complexes (R = H, F, CH_3) in order to study the insertion of propene in the Pt−H bond. In general, insertion and β-elimination barriers tend to be small. Insertion barriers of about 10 kJ/mol are found for R = H and 3−9 kJ/mol for R = CH_3, and an almost negligible insertion barrier appears for R = F (2−4 kJ/mol). Since propene insertion can generate both linear propyl and branched isopropyl complexes, it is possible to study the distribution between these two complexes, which is of importance for catalyst selectivity. It turns out that linear complexes are favored over branched ones, in agreement with available experimental data. The energy gap between the two forms decreases in the order R = Me > R = H > R = F. Another point of interest is the double-bond isomerization of propene which can arise from isopropyl complexes. Two pathways are identified: a direct exchange of β-hydrogens in the β-agostic isopropyl complex ("isopropyl rock") and a process in which isomerization occurs by association and dissociation of a coordinating solvent molecule (acetonitrile was used in the present study). Which one of these two processes dominates seems to depend on the nature of the solvent and the substituents on the phosphines. Even though very few experimental data are available, a satisfying agreement is found between optimized geometries and X-ray data of a related compound as well as between computed and experimental product distributions. The calculated "isopropyl rock" barriers are also in accord with recent NMR measurements from which the barrier could be determined. Finally, a crude estimate of the isomerization rate seems to agree with the theoretical predictions.

1. Introduction

Multistep catalytic reactions, such as olefin hydrogenation, hydroformylation, or isomerization, involve the migratory insertion of an olefin into the metal−hydrogen (M−H) bond as a key step in the catalytic cycle.[1,2] Concerning Pt(II) complexes, Chatt and Shaw[3] first reported the thermolysis of *trans*-$PtL_2(Et)Cl$ giving *trans*-$PtL_2(H)Cl$ and ethene by β-elimination (L = PEt_3), which is the reverse reaction of olefin insertion. Since then, several studies have appeared attempting to clarify the detailed mechanism of the insertion/β-elimination reaction.[4−9] It is generally accepted by now that, for cationic Pt(II) complexes, insertion proceeds through a 4-coordinate intermediate of the type [Pt-$(PR_3)_2H(olefin)^+$].[14,18] Note that, for insertion or β-elimination to occur, the olefin and the hydride ligand need to be in a cis, coplanar coordination, as shown in Scheme 1.

For several platinum−phosphine−hydride complexes, however, the isomer having the phosphine ligands in trans position is known to be more stable than the cis analogue. Hence, a trans to cis isomerization should

[†] University of Leuven.
[‡] DSM Research.

(1) Collmann, J. P.; Hegedus, L. S.; Norton, J. R.; Finke, R. C. *Principles and Applications of Organotransition Metal Chemistry*; University Science Books: Mill Valley, CA, 1987; Chapter 6.
(2) Crabtree, R. H. *The Organometallic Chemistry of the Transition Elements*; Wiley: New York, 1988; Chapter 7.
(3) Chatt, J.; Shaw, B. L. *J. Chem. Soc.* **1962**, 5075.
(4) Clark, H. C.; Kurosawa, H. *Inorg. Chem.* **1972**, *11*, 1275.
(5) Clark, H. C.; Jablonski, C. R. *Inorg. Chem.* **1974**, *13*, 2213.
(6) Clark, H. C.; Wong, C. S. *J. Am. Chem. Soc.* **1974**, *96*, 7213.
(7) Clark, H. C.; Jablonski, C. R. *Inorg. Chem.* **1975**, *14*, 1332.
(8) Bracher, G.; Pregosin, P. S.; Venanzi, L. M. *Angew. Chem., Int. Ed. Engl.* **1975**, *14*, 563.
(9) Brainard, R. L.; Whitesides, G. M. *Organometallics* **1985**, *4*, 1550.
(10) Alibrandi, G.; Minniti, D.; Scolaro, L. M.; Romeo, R. *Inorg. Chem.* **1988**, *27*, 318.
(11) Alibrandi, G.; Cusumano, M.; Minniti, D.; Scolaro, L. M. *Inorg. Chem.* **1989**, *28*, 342.
(12) Alibrandi, G.; Scolaro, L. M.; Minniti, D.; Romeo, R. *Inorg. Chem.* **1990**, *29*, 3467.
(13) Alibrandi, G.; Scolaro, L. M.; Romeo, R. *Inorg. Chem.* **1991**, *30*, 4007.
(14) Romeo, R.; Alibrandi, G.; Scolaro, L. M. *Inorg. Chem.* **1993**, *32*, 4688.
(15) Romeo, R.; Alibrandi, G. *Inorg. Chem.* **1997**, *36*, 4822.
(16) Romeo, R.; Plutino, M. R.; Elding, L. I. *Inorg. Chem.* **1997**, *36*, 5909.
(17) Carr, N.; Dunne, B. J.; Orpen, A. G.; Spencer, J. L. *J. Chem. Soc., Chem. Commun.* **1988**, 926.
(18) Mole, L.; Spencer, J. L. *Organometallics* **1991**, *10*, 49.

10.1021/om9806895 CCC: $18.00
Publication on Web 04/24/1999

Scheme 1

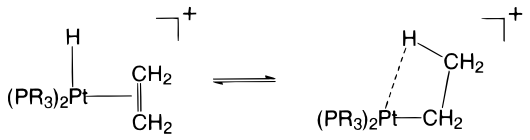

take place before insertion or elimination can proceed. The mechanism of the isomerization reaction has also received considerable interest in the past few years.[10−16] However, the cis−trans isomerization can be avoided by using a chelating bis-phosphine ligand. As a matter of fact, the equilibrium of Scheme 1 has recently been demonstrated by Spencer et al. by making use of bis-phosphine ligands.[17−20] These authors isolated and characterized the Pt−alkyl form obtained after insertion, clearly showing the presence of a β-agostic interaction between Pt and the β-hydrogen on the alkyl ligand. If higher homologues of ethene are involved, the insertion can lead to a mixture of different alkyl metal complexes, and the various isomers and their relative stabilities often control the outcome of a catalytic reaction.[21−24] Scheme 2 shows the two possible complexes obtained after insertion of propene in the Pt(II)−H bond. Only the branched alkyl product can then proceed to isomerization of the double bond.

Although a number of theoretical studies were performed on the insertion/elimination reaction of Pt(II) complexes,[25−30] the effect of differently substituted phosphines on the energy barriers has been investigated in a very preliminary way only,[25] and no results are available on the insertion of higher olefins. Therefore, the present work investigates the insertion of propene in $Pt(PR_3)_2H^+$, for R = H, F, and CH_3. Apart from yielding a more realistic model, the larger olefin also allows studying the double-bond isomerization reaction and the relative stabilities of branched and linear alkyl complexes.

2. Computational Details

Both classical ab initio and density functional theory (DFT) calculations have been carried out on the species of interest. The classical ab initio calculations include RHF theory followed by a second-order perturbation treatment (MP2). On the DFT side, the B3PW91 hybrid functional was used. For the exchange part, this functional consists of a mixture of Slater exchange, E_X^{LSDA}, Hartree−Fock exchange, E_X^{exact}, and Becke's 1988 gradient correction to the exchange,[31] E_X^{B88}. The correlation part is a combination of the exact correlation of the homogeneous electron gas, E_C^{LSDA},[32] and a gradient correction provided by Perdew and Wang,[33] ΔE_C^{PW91}. The coefficients of the various contributions were optimized by Becke via fitting to atomization energies, ionization potentials, proton affinities, and atomic energies in the G1 molecule set.[34]

Geometries were optimized using both RHF and B3PW91, with convergence thresholds of 0.0005 hartree/bohr for the maximum gradient, 0.0005 bohr for the maximum displacement, and 10^{-5} hartree for the maximum energy change. Single-point MP2 calculations were done on both optimized HF and B3PW91 geometries. All calculations were carried out using the same basis set, i.e., a DZP basis on all nonmetal atoms, and for the larger molecular systems, a DZ basis on less important portions of the molecule (methyl groups and F atoms). For Pt, 60 core electrons were replaced by an averaged relativistic effective potential, with the remaining valence space of Pt (5s, 5p, 5d, 6s, 6p) represented by a (5s5p4d)/[4s3p3d] basis.[35] In one case, a few QCISD calculations have been carried out as well, making use of the B3PW91 optimized geometries. For these calculations, the DZP basis set was placed on all atoms, except for the phosphine hydrogens. The latter atoms were treated with a DZ basis for reasons of computational cost.

Concerning the location of transition structures for insertion, a stepwise procedure was used initially at the HF level. The distance between the attacking carbon and the hydride ligand was kept frozen at approximately five values in the range 1.4−2.0 Å, while the remaining geometrical parameters were relaxed. For the structure with the highest energy a numerical frequency calculation was done, producing a Hessian used as starting point for full HF optimization to a transition state. The updated HF Hessian produced in the latter run served as a starting Hessian for B3PW91 full TS optimizations.

All these calculations were performed using the Turbomole 96.0 program as implemented in the MSI suite of molecular modeling tools.[36]

In a few cases, the influence of solvent effects has been studied using the self-consistent isodensity polarized continuum model (SCI−PCM) as implemented in the GAUSSIAN-94 package.[37] The SCI−PCM method treats the molecule under consideration by putting it in a cavity with molecular shape (determined by an isodensity surface) embedded in a continuous medium. This continuous medium is characterized only by its dielectric constant, ϵ. The SCI−PCM calculations were performed at the HF and B3PW91 level of theory using the default isodensity value of 0.0004 e/bohr^3. Geometries were taken from the Turbomole calculations, and the same basis sets were employed as described above.

Throughout the text, relative energies are in kJ/mol, distances in angstroms, and angles in degrees.

3. Results and Discussion

Figure 1 shows schematic representations of the three most important structures involved in the insertion of

(19) Carr, N.; Dunne, B. J.; Mole, L.; Orpen, A. G.; Spencer, J. L. *J. Chem. Soc., Dalton Trans.* **1991**, 863.
(20) Carr, N.; Mole, L.; Orpen, A. G.; Spencer, J. L. *J. Chem. Soc., Dalton Trans.* **1992**, 2653.
(21) Slaugh, L. H.; Mullineaux, R. D. *J. Organomet. Chem.* **1968**, *13*, 469.
(22) Evans, D.; Osborn, J. A.; Wilkinson, G. *J. Chem. Soc. A* **1968**, 3133.
(23) Orchin, M.; *Adv. Catalysis*, **1966**, *16*, 1.
(24) Tolman, C. A. *J. Am. Chem. Soc.* **1972**, *94*, 2994.
(25) Coussens, B. B.; Buda, F.; Oevering, H.; Meier, R. J. *Organometallics* **1998**, *17*, 795.
(26) Rocha, W. R.; De Almeida, W. B. *Organometallics* **1998**, *17*, 1961.
(27) Sakaki, S.; Ogawa, M.; Musashi, Y.; Arai, T. *J. Am. Chem. Soc.* **1994**, *116*, 7258.
(28) Thorn, D. L.; Hoffmann, R. *J. Am. Chem. Soc.* **1978**, *100*, 2079.
(29) Armstrong, D. R.; Fortune, R.; Perkins, P. G. *J. Catal.* **1976**, *41*, 51.
(30) Sakaki, S.; Kato, H.; Kanai, H.; Tarama, K. *Bull. Chem. Soc. Jpn.* **1975**, *48*, 813.
(31) Becke, A. D. *J. Chem. Phys.* **1988**, *88*, 1053.
(32) Vosko, S. J.; Wilk, L.; Nusair, M. *Can. J. Phys.* **1980**, *58*, 1200.
(33) Perdew, J. P.; Wang, Y. *Phys. Rev. B* **1992**, *45*, 13244.
(34) Becke, A. D. *J. Chem. Phys.* **1993**, *98*, 5648.
(35) Ross, R. B.; Powers, J. M.; Atashroo, T.; Ermler, W. C. *J. Chem. Phys.* **1990**, *93*, 6654.
(36) Computational results obtained using software programs from Molecular Simulations; the calculations were done with the Turbomole program.
(37) Frisch, M. J.; Trucks, G. W.; Schlegel, H. B.; Gill, P. M. W.; Johnson, B. G.; Robb, M. A.; Cheeseman, J. R.; Keith, T. A.; Petersson, G. A.; Montgomory, J. A.; Raghavachari, K.; Al-Laham, M. A.; Zakrzewski, V. G.; Ortiz, J. V.; Foresman, J. B.; Cioslowski, J.; Stefanov, B. B.; Nanayakkara, A.; Challacombe, M.; Peng, C. Y.; Ayala, P. Y.; Chen, W.; Wong, M. W.; Andres, J. L.; Replogle, E. S.; Gomperts, R.; Martin, R. L.; Fox, D. J.; Binkley, J. S.; Defrees, D. J.; Baker, J.; Stewart, J. P.; Head-Gordon, M.; Gonzalez, C.; Pople, J. A. *Gaussian94* (Revision E.2); Gaussian, Inc.: Pittsburgh, PA, 1995.

Scheme 2

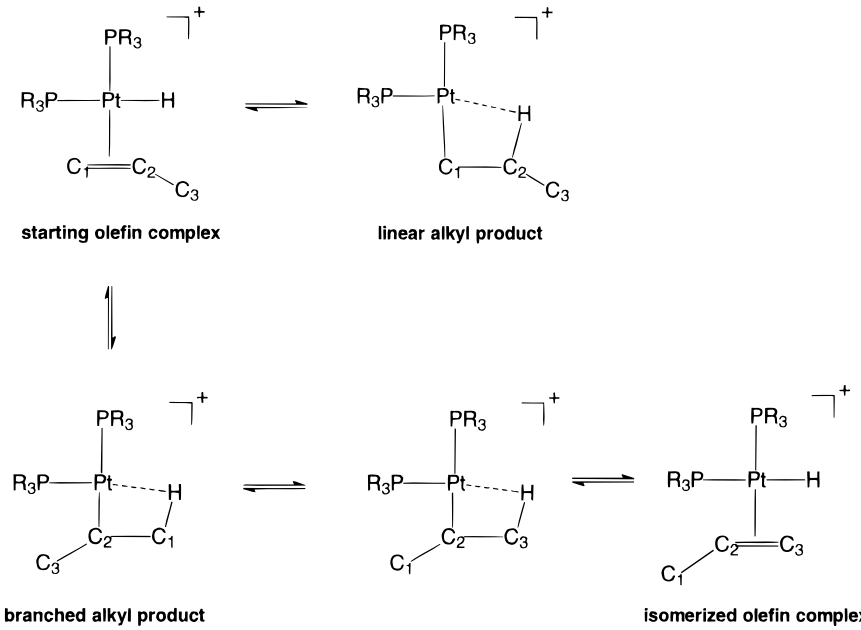

propene in the Pt−H bond: the reactant state (R) having a π-coordinated olefin, the transition state (TS) for insertion, and the product propyl complex (P) involving a β-agostic Pt−H interaction. As already outlined in the Introduction, two different insertion products can be obtained. If the carbon atom bearing a CH_3 group ($R_1 = H$, $R_2 = CH_3$) attacks the hydride, a linear propyl ligand ($-CH_2-CH_2-CH_3$, Pr) is obtained, whereas insertion of propene via the other carbon ($R_1 = CH_3$, $R_2 = H$) yields an isopropyl ligand ($-CH(CH_3)_2$, *i*-Pr). Throughout this paper, these two olefin complex conformations, as well as the transition structures and alkyl complexes derived from them, will be denoted A and B, respectively. Furthermore, the different rotational conformations of the phosphine groups, also shown in Figure 1, are numbered 1 to 6. Note, however, that the six conformers do not represent an exhaustive list, but rather a sufficient number of rotational conformations to describe our findings. Shorthand notations are used in the following sections, such as TS-A1, designating a transition state, having conformation A for the olefin and 1 for the phosphines.

For reasons of computational cost, only a limited number of structures has been considered at all levels of theory. The general strategy adopted was to optimize the different conformations at the HF level, followed by reoptimization of the most relevant species using the B3PW91 functional. For the sake of simplicity, only the most stable and important molecules will be presented in the tables. It should be noted at this point that all reagent (R) and product (P) structures possess C_1 symmetry and that the geometry optimizations have been carried out without any constraints. Therefore, although no vibrational analyses were performed for reagent and product structures, it is most likely that all of them can be regarded as true minima on the potential energy surface.

3.1. Insertion of Propene in Pt(PH$_3$)$_2$H$^+$. 3.1.1. Geometries. Table 1 contains geometrical parameters for the most important structures involved in the insertion of propene in Pt(PH$_3$)$_2$H$^+$, whereas Table 2 lists the respective relative energies. Similar to our previous work on ethene insertion,[25] the R-A1 form turns out to be the most stable π-complex. In the alternative R-B conformation, the P_2-phosphine is slightly rotated due to steric hindrance with the CH_3 group of propene. Therefore, R-B6 is the most stable B-conformation. The fact that R-B6 suffers steric hindrance is also clearly seen from the H−Pt−C_1−C_2 dihedral angle. This angle is 6.1° (HF) or 7.6° (B3PW91) in R-A1, indicating that the olefin is oriented nearly parallel to the Pt−H bond, whereas in R-B6 it amounts to −18.5° (HF) or −17.1° (B3PW91). Starting from R-A1 and R-B6, insertion proceeds through TS-A1 and TS-B6, yielding the product alkyl complexes P-A1 and P-B1, respectively. P-B1 is obtained as direct product, and not P-B6, indicating that steric hindrance between the P_2-phosphine and the methyl group of propene is reduced on going from R-B to P-B. Indeed, the H−Pt−C_1−C_2 angles of the product complexes are smaller than those of reactants or transition structures.

Due to the trans influence of the hydride ligand in the π-complex, the Pt−P_2 bond is 0.15 Å longer than the Pt−P_1 bond. In the transition states, these bonds are quite similar, while the reverse situation occurs for the corresponding product complexes. These observations are in agreement with the simultaneous breaking of the Pt−H bond and the formation of a Pt−C_1 bond. During the insertion, the C_1−C_2 bond elongates by about 0.1 Å, indicating the diminishing double-bond character. For the HF-optimized geometries, the C_2−H distance in the transition states is found to be 1.548 Å (TS-A1) and 1.580 Å (TS-B6). B3PW91 leads to longer bonds of 1.646 and 1.640 Å, respectively. Note that the C_2−H bond in the product complexes is relatively long, more than 1.2 Å, which is a consequence of the β-agostic interaction. Closer examination of Table 1 shows that in P-A1 the C_2−H bond is 0.04 Å longer than in P-B1. This is probably due to the fact that C_2 in P-A1 is a

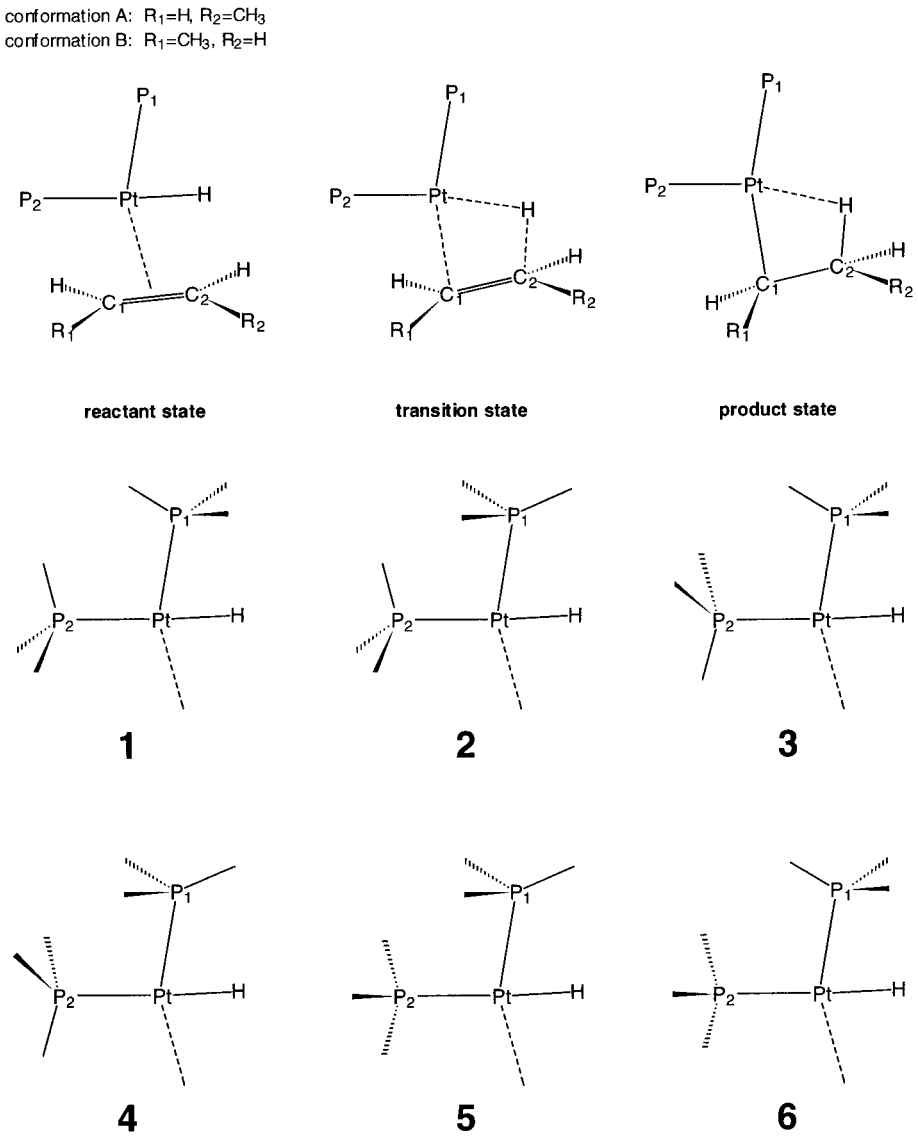

Figure 1. Schematic representations of the structures involved in the insertion of propene in the Pt−H bond.

Table 1. Optimized Geometrical Parameters of $Pt(PH_3)_2H^+$ Related Species (Angles in deg, Distances in Å; See Figure 1 for Shorthand Notations of the Structures and Atom Definitions)

PH_3		Pt−P_1	Pt−P_2	Pt−C_1	Pt−H	C_1−C_2	C_2−H	P_1−Pt−P_2	P_1−Pt−H	P_2−Pt−C_1	H−Pt−C_1−C_2
R-A1	HF	2.313	2.450	2.322	1.575	1.362	2.317	98.6	79.5	84.4	6.1
	B3PW91	2.284	2.374	2.231	1.594	1.392	2.183	97.7	78.5	84.5	7.6
TS-A1	HF	2.385	2.377	2.135	1.643	1.424	1.548	100.4	89.6	93.4	2.5
	B3PW91	2.314	2.331	2.154	1.633	1.423	1.646	99.2	87.3	92.2	4.2
P-A1	HF	2.434	2.322	2.078	1.779	1.473	1.255	101.5	94.2	95.0	2.1
	B3PW91	2.352	2.281	2.098	1.766	1.469	1.283	101.4	93.8	94.4	−1.1
R-B6	HF	2.311	2.463	2.427	1.571	1.356	2.334	97.5	78.3	84.2	−18.5
	B3PW91	2.287	2.379	2.309	1.591	1.388	2.206	97.0	77.8	83.9	−17.1
TS-B6	HF	2.382	2.388	2.177	1.628	1.413	1.580	99.7	88.2	93.1	−3.1
	B3PW91	2.319	2.337	2.196	1.628	1.420	1.640	98.8	86.5	91.7	−4.7
P-B1	HF	2.450	2.318	2.084	1.823	1.482	1.214	101.4	94.5	95.1	2.8
	B3PW91	2.358	2.273	2.114	1.799	1.476	1.239	100.9	93.8	95.0	−1.2

PH_3		Pt−P_1	Pt−P_2	Pt−C_1	Pt−C_2	Pt−N	N−C	P_1−Pt−P_2	P_1−Pt−N	P_2−Pt−C_1	P_2−Pt−C_2
P-A1-MeCN	HF	2.486	2.283	2.102		2.136	1.127	99.3	90.0	83.7	
	B3PW91	2.394	2.241	2.115		2.062	1.152	98.6	91.1	83.4	
P-B1-MeCN	HF	2.492	2.285		2.119	2.140	1.127	97.7	87.9		84.8
	B3PW91	2.407	2.244		2.137	2.066	1.152	97.7	89.3		84.3

secondary carbon (in contrast to a primary carbon in P-B1) and thus more able to release a hydride.

To our knowledge, there is only one X-ray diffraction experiment available on cationic Pt(II) complexes where the Pt−H β-agostic interaction was actually seen.[17] It concerns the molecule $(Bu^t_2P(CH_2)_2PBu^t_2)Pt(norbornyl)^+$. Due to the bis-phosphine ligand, this system has a bite angle of only 89.3°. Even though this angle is about 11° smaller than in P−A1 and P−B1, it still seems useful to compare calculated values with the other structural

Table 2. Relative Energies (kJ/mol) of the Pt(PH$_3$)$_2$H$^+$ Related Species (See Figure 1 for the Shorthand Notation of the Structures)

	HF	MP2// HF	B3PW91	MP2// B3PW91	QCISD// B3PW91
Pt(PH$_3$)$_2$H$^+$ + Propene reaction[a]					
R-A1	0.0	0.0	0.0	0.0	0.0
R-B6	8.7	2.8	5.0	1.7	4.0
R-C	6.1	10.9	9.4	12.7	
R-D	4.8	9.6	8.0	11.0	
TS-A1	20.8	1.5	7.5	10.6	13.5
TS-B6	33.2	3.5	13.9	12.3	19.4
P-A1	15.0	−1.1	1.7	8.3	9.9
P-B1	19.5	−1.2	1.8	1.7	11.3
Insertion Barrier/Elimination Barrier					
TS-A1	20.8/5.8	1.5/2.6	7.5/5.8	10.6/2.3	13.5/3.6
TS-B6	24.5/13.7	0.7/4.7	8.9/12.1	10.6/10.6	15.4/8.1
Rotation Barrier R-A1 → R-B6					
45°[b]	17.0	20.0	19.1	20.2	
225°[b]	10.3	15.8	13.0	16.0	
Rotation Barrier P-B1 → P-B1					
0°[c]	35.8	67.7	47.1	66.7	
150°[c]	46.8	80.6	60.9	81.6	
Products Pt(PH$_3$)$_2$(propyl)(CH$_3$CN)$^+$[d]					
P-A1-MeCN	0.0	0.0	0.0	0.0	
P-B1-MeCN	10.3	−1.9	4.9	−2.2	

[a] Relative energy with respect to R-A1. [b] Relative energy with respect to R-A1; see text for angle definition. [c] Relative energy with respect to P-B1; see text for angle definition. [d] Relative energy with respect to P-A1-MeCN.

parameters. In fact, as shown in the table below, the agreement between the calculated and experimental geometries is quite good. Furthermore, the B3PW91 values seem to be in better agreement with experiment than the HF values.

	expt	P-A1 calc HF	P-A1 calc B3PW91	P-B1 calc HF	P-B1 calc B3PW91
Pt-P$_1$	2.311	2.434	2.352	2.450	2.358
Pt-P$_2$	2.256	2.322	2.281	2.318	2.273
Pt-C$_1$	2.096	2.078	2.098	2.084	2.114
Pt-H	1.907	1.779	1.766	1.823	1.799
C$_2$-H	1.286	1.255	1.283	1.214	1.239
C$_1$-C$_2$	1.480	1.473	1.469	1.482	1.476

An important parameter for the design of catalysts containing a chelating bis-phosphine ligand is the P$_1$−Pt−P$_2$ bite angle. Table 1 shows that this angle remains almost unaffected during the insertion process, being smallest for the reactant π-complexes (97−99°) and opening up by only 3−4° in the product complexes. These results are in clear contrast with the extended Hückel results of Thorn and Hoffmann,[28] who reported an angle change from 95° to 110° for ethene insertion.

3.1.2. Energetics. Generally, insertion barriers tend to be low. For the A1 and B6 conformations, HF yields values of 20.8 and 24.5 kJ/mol, respectively, while the B3PW91 values are considerably lower (7.5 and 8.9 kJ/mol). MP2 single-point calculations at both the HF and B3PW91 geometries shed some more light on this point. Barriers calculated at the MP2//HF level of theory amount to only 1.5 and 0.7 kJ/mol for the TS-A1 and TS-B6 insertion, thus implying a dramatic decrease. However, if applied on the B3PW91 geometries, a value of 10.6 kJ/mol is obtained for both energy barriers. It seems that the high barriers at the HF level should mainly be attributed to the lack of correlation effects. Qualitatively, A1 inserts more easily than B6 at both the HF and B3PW91 levels of theory, which is in contrast to MP2//HF calculations suggesting a reverse situation. Note, however, that the differences in barrier heights are rather small for the latter method. At the MP2//B3PW91 level, both insertions even have the same energy barrier. The barrier heights for the reverse β-elimination reaction (P→TS→R) are also given in Table 2. While for P-A1 the elimination barrier is relatively low, P-B1 seems somewhat more resistant toward β-elimination.

Concerning the β-agostic product complexes, HF predicts P-A1 to be more stable than P-B1 by 4.5 kJ/mol. B3PW91 and MP2//HF, on the other hand, yield equally stable products, and at the MP2//B3PW91 level the branched P-B1 complex turns out to be lower in energy than the linear P-A1. The relative stabilities of the products are considered in more detail in a following section.

Due to the difference in relative energies as obtained by the above-mentioned computational methods, a few QCISD calculations have been carried out as well, making use of the B3PW91 optimized geometries. The DZP basis set was placed on all atoms, except for the phosphine hydrogens, which were treated with a DZ basis, for reasons of computational cost. The resulting relative energies are shown in Table 2. It is clearly seen now that, for relative energies (R-A1 versus R-B6, TS-A1 versus TS-B6 and P-A1 versus P-B1), the B3PW91 results compare very well to the QCISD ones, in contrast to the MP2//B3PW91 calculations. For the relative stability of P-A1 versus P-B1, MP2 yields qualitatively incorrect results as compared to QCISD. In an absolute energetic sense, it cannot be stated which of the two methods (B3PW91 or MP2) agrees better with QCISD. Concerning the energy barriers for insertion, it is seen that, although the MP2 energies are closer to the QCISD ones, B3PW91 yields the correct qualitative behavior. For elimination barriers, the three methods yield an analogous trend.

3.1.3. Comparison with the Pt(PH$_3$)$_2$H$^+$−Ethene System. As already mentioned, the insertion reaction of ethene in Pt(PH$_3$)$_2$H$^+$ has been investigated in a previous study.[25] For the sake of comparison we recomputed the most important stationary points using the same computational methods presently used for the propene insertion. Tables 3 and 4 contain both the latter results and the ones obtained previously for geometries and energies, respectively. As expected, MP2//B3PW91 relative energies are very close to the MP2//MP2 values. This indicates that MP2 and B3PW91 geometries are rather close to each other, which can also be seen from Table 3. It seems however, that the strength of the β-interaction at the B3PW91 level of theory is somewhat underestimated with respect to the MP2//MP2 level, as can be seen from the slightly shorter Pt−H distance obtained by the latter method for the product complex P-1. Similarly, the C$_2$−H distance in the product ethyl complex is longer at the MP2 level (1.270 Å) as compared to the B3PW91 level (1.247 Å). The strength of the β-agostic interaction can also be estimated by the energy difference between P-1 and P-1-rot. Since the latter structure is in fact a transition state for rotation of the methyl group of ethylene (interchanging the β-hydrogens), its barrier is mainly determined by the

Table 3. Optimized Geometrical Parameters of the Species Related to Ethene Insertion in $Pt(PH_3)_2H^+$ (Angles in deg, Distances in Å; See Figure 1 for Shorthand Notations of the Structures and Atom Definitions)

		Pt−P_1	Pt−P_2	Pt−C_1	Pt−H	C_1−C_2	C_2−H	P_1−Pt−P_2	P_2−Pt−C_1
R-1	HF	2.314	2.451	2.348	1.575	1.357	2.276	99.0	83.5
	MP2	2.283	2.369	2.224	1.571	1.385	2.166	97.6	82.5
	B3PW91	2.290	2.373	2.245	1.595	1.388	2.151	98.2	83.5
TS-1	HF	2.376	2.384	2.159	1.632	1.410	1.591	100.2	92.6
	MP2[a]	2.310	2.332	2.155	1.608	1.421	1.600	99.8	90.5
	B3PW91	2.313	2.337	2.170	1.628	1.414	1.676	99.0	91.0
P-1	HF	2.440	2.314	2.072	1.826	1.473	1.220	101.1	94.6
	MP2	2.340	2.278	2.102	1.732	1.467	1.270	100.4	94.3
	B3PW91	2.353	2.271	2.095	1.794	1.470	1.247	100.5	95.1

[a] Constrained optimization with C_2−H frozen to 1.600 Å.

Table 4. Relative Energies (kJ/mol) of the Species Related to Ethene Insertion in $Pt(PH_3)_2H^+$ (See Figure 1 for the Shorthand Notation of the Structures)

	HF// HF	MP2// MP2	BLYP// BLYP	BPW// BPW	MP2// HF	B3PW91// B3PW91	MP2// B3PW91
R-1	0.0	0.0	0.0	0.0	0.0	0.0	0.0
TS-1	18.2	10.9	11.3	6.7	2.0	6.3	9.9
P-1	5.4	4.6	0.4	−4.6	−3.1	−5.9	4.5
P-1 rot[a]	37.3	64.0	33.1	35.1	63.8	37.7	63.4
trans-P[b]	4.2				29.5	16.7	40.6

[a] Transition state for rotation of the methyl group. [b] *trans*-$Pt(PH_3)_2H(ethyl)^+$.

strength of the β-interaction. While the MP2//B3PW91 method yields 58.9 kJ/mol for this barrier, it is only 43.6 kJ/mol at the B3PW91 level, indicating a reduced β-interaction at the latter level of theory. The obtained barriers for ethene insertion range from 6.3 to 10.9 kJ/mol (excluding HF results), almost identical to the barriers for the propene A1 and B6 insertions.

3.2. Effect of PF_3 and PMe_3 Substitution. For the calculations of complexes containing larger phosphines, the F atoms in PF_3 and the methyl groups in PMe_3 were treated with the smaller DZ basis set in order to speed up the calculations. The most important geometrical data for the PF_3 and PMe_3 complexes are summarized in Tables 5 and 7, whereas Tables 6 and 8 contain the corresponding relative energies. Similar to the $Pt(PH_3)_2H^+$ species, HF calculations suggest the conformations R-A1 and R-B6 being the most stable for F-containing species. These reactant π-complexes correlate to the products P-A1 and P-B6 through transition states TS-A1 and TS-B1, respectively. A different situation arises for PMe_3 substitution. Due to obvious steric interactions between the methyl groups, rotational conformations 1 and 4 are destabilized (see Figure 1). The energy difference between conformations 2 and 3, however, is rather small. Therefore, the latter rotational conformations were considered at all levels of theory for the reactant states. It turned out, then, that HF predicts R-A3 to be the more stable π-complex, while it is R-A2 at the B3PW91 level of theory. Concerning the B-forms, all methods uniformly favor R-B5 over R-B3. Note that R-B5 is obtained instead of R-B2 for similar steric interactions as mentioned in a previous section on PH_3 complexes. R-B5 correlates to TS-B5, which could be located at all levels of theory. In contrast, for the R-A conformations, only the transition states correlating to the most stable reactant could be found, within a certain level of theory. Thus, TS-A3 was located at the HF level but not when using B3PW91, and similarly, a TS derived from R-A2 (TS-A5) could only be found with the B3PW91 method. For the relative stabilities of the product alkyl complexes P-A2 and P-A3, all methods turn out to be in good agreement. In contrast, P-B5 is predicted to be more stable than P-A2 and P-A3 at the MP2//B3PW91 level of theory, while the reverse trend occurs when using the B3PW91 method.

For the Pt−P and C_1−C_2 distances the same trends are seen as in the PH_3 case, although the actual Pt−PF_3 distances are somewhat shorter than for the PH_3-containing complexes (shortening of about 0.06−0.07 Å), whereas the average Pt−PMe_3 distance is 0.016 Å longer than its Pt−PH_3 analogue. The C_2−H distance in the transition state for insertion in $Pt(PF_3)_2H^+$ amounts to 1.484 (TS-A1) and 1.590 Å (TS-B1) at the HF level. Similar to the case with PH_3 ligands, B3PW91 yields longer C_2−H bonds of 1.703 and 1.734 Å, respectively. This is also observed for TS-B5 of the PMe_3-containing systems. Note, however that, whereas the elongation of the C_2−H bond distances when going from HF to B3PW91 is moderate for PH_3 and PMe_3 complexes (up to 0.1 Å), it is quite severe in the case of PF_3 complexes (up to 0.2 Å).

Compared to the PH_3 analogues, the bite angle is about 3−4° larger for fluorine- and methyl-containing systems. Obviously, this is due to the stronger steric hindrance between these larger phosphines. The change of this angle during the insertion process is quite similar (about 4°).

More interesting, from an experimental point of view, is the effect of electron-donating and -withdrawing groups on the energetics of the insertion. The relative stability of R-A versus R-B forms turns out to be more or less constant throughout the series of PH_3, PF_3, and PMe_3 complexes. The insertion barriers, on the other hand, vary considerably. First we note that, in the case of PF_3 and PMe_3, MP2//HF yields negative barriers, in contrast to MP2//B3PW91, which indicates a deficiency of the HF geometries. Thus, since HF geometries seem inaccurate, the reliability of the HF energies is also questionable. Therefore, we focus our attention only on the B3PW91 and MP2//B3PW91 levels of theory. While an insertion barrier of about 8−11 kJ/mol exists for PH_3-containing complexes, it is only 3−9 kJ/mol for the PMe_3-substituted species, and insertion becomes almost barrierless for PF_3 complexes (barriers of about 2−4 kJ/mol). Thus, even though the differences are small, a clear trend of decreasing insertion barriers is found through the series $PH_3 > PMe_3 > PF_3$. In all cases, the insertion of propene in the R-A form turns out to be slightly more difficult than in the R-B form. For

Table 5. Optimized Geometrical Parameters of Pt(PF$_3$)$_2$H$^+$ Related Species (Angles in deg, Distances in Å; See Figure 1 for Shorthand Notations of the Structures and Atom Definitions)

PF$_3$		Pt−P$_1$	Pt−P$_2$	Pt−C$_1$	Pt−H	C$_1$−C$_2$	C$_2$−H	P$_1$−Pt−P$_2$	P$_1$−Pt−H	P$_2$−Pt−C$_1$	H−Pt−C$_1$−C$_2$
R-A1	HF	2.249	2.375	2.296	1.579	1.372	2.264	102.6	79.4	84.3	10.6
	B3PW91	2.222	2.300	2.236	1.603	1.394	2.131	102.2	79.5	84.4	10.6
TS-A1	HF	2.324	2.298	2.134	1.661	1.432	1.484	103.6	90.1	92.2	2.5
	B3PW91	2.247	2.276	2.174	1.632	1.418	1.703	102.7	86.2	90.2	6.0
P-A1	HF	2.352	2.270	2.105	1.729	1.456	1.319	103.9	92.7	93.0	1.9
	B3PW91	2.282	2.227	2.116	1.751	1.461	1.303	104.0	92.6	93.0	3.0
R-B6	HF	2.245	2.388	2.438	1.573	1.361	2.291	100.0	78.2	83.3	−16.0
	B3PW91	2.226	2.311	2.344	1.598	1.388	2.151	100.3	78.4	83.3	−14.3
TS-B1	HF	2.309	2.319	2.203	1.627	1.411	1.590	102.4	87.9	91.5	−4.2
	B3PW91	2.247	2.284	2.246	1.621	1.410	1.734	100.9	85.7	89.4	−3.6
P-B1	HF	2.374	2.256	2.116	1.790	1.469	1.237	102.9	94.4	93.6	−1.5
	B3PW91	2.294	2.221	2.141	1.796	1.470	1.246	102.7	93.8	93.7	−2.7

PF$_3$		Pt−P$_1$	Pt−P$_2$	Pt−C$_1$	Pt−C$_2$	Pt−N	N−C	P$_1$−Pt−P$_2$	P$_1$−Pt−N	P$_2$−Pt−C$_1$	P$_2$−Pt−C$_2$
P-A1-MeCN	HF	2.428	2.209	2.111		2.123	1.127	102.3	87.3	83.9	
	B3PW91	2.331	2.181	2.134		2.075	1.152	101.4	89.4	83.3	
P-B1-MeCN	HF	2.447	2.205		2.138	2.134	1.128	101.1	86.7		83.3
	B3PW91	2.346	2.178		2.165	2.082	1.152	101.2	88.0		82.5

Table 6. Relative Energies (kJ/mol) of the Pt(PF$_3$)$_2$H$^+$ Related Species (See Figure 1 for the Shorthand Notation of the Structures)

	HF	MP2//HF	B3PW91	MP2//B3PW91
Pt(PF$_3$)$_2$H$^+$ + Propene Reaction[a]				
R-A1	0.0	0.0	0.0	0.0
R-B6	11.1	2.1	5.7	0.8
TS-A1	16.7	−4.7	1.8	2.7
TS-B1	28.2	−1.3	8.5	4.5
P-A1	15.8	−7.2	−3.4	−2.1
P-B6	18.5	−10.6	−6.7	−5.4
Insertion Barrier/Elimination Barrier				
TS-A1	16.7/0.9	−4.7/2.5	1.8/5.2	2.7/4.8
TS-B1	17.7/9.7	−3.4/9.3	2.8/15.2	3.7/9.9
Rotation Barrier P-B1 → P-B1				
0°[b]	49.4	71.2	44.4	54.2
Products Pt(PF$_3$)$_2$(propyl)(CH$_3$CN)$^+$[c]				
P-A1-MeCN	0.0	0.0	0.0	0.0
P-B1-MeCN	8.7	−3.2	2.6	−4.1

[a] Relative energy with respect to R-A1. [b] Relative energy with respect to P-B1; see text for angle definition. [c] Relative energy with respect to P-A1-MeCN.

elimination barriers, no clear trends can be observed with regard to electron-donating or -withdrawing groups, but similarly to insertion, elimination is considerably facilitated when starting from linear propyl complexes (P-A forms). While for PH$_3$, the direct β-agostic products are less stable than the reactant olefin complexes, the reverse is seen for PF$_3$. For PMe$_3$, it seems to depend on the employed method whether the alkyl form is more stable than the olefin-hydride form or not. Concerning the product distributions, a more detailed discussion is given in a following section.

3.3. Double-Bond Isomerization of Propene. 3.3.1. Rotation around the Pt−[olefin] Bond in the Reactant Pt(PH$_3$)$_2$(propene)$^+$ π-Complex. As outlined in the Introduction, only branched insertion products can undergo double-bond isomerization. To obtain a branched alkyl structure (isopropyl ligand), the π-complex should possess the B-conformation. Therefore, the olefin may either coordinate directly in this way or undergo rotation starting from conformation A. To investigate rotation around the Pt−[olefin] bond, a number of constrained optimizations were carried out at the HF level for the Pt(PH$_3$)$_2$(propene)$^+$ system. Figure 2 shows the rotational potential energy profile obtained by constraining the H−Pt−C$_1$−C$_2$ angle of R-A1 at various values and relaxing the other geometrical parameters (see Figure 1 for atom definitions). The highest relative energy during rotation amounts to about 17 kJ/mol (HF) and corresponds to a structure with high repulsion between the methyl group of propene and the P$_2$-phosphine (H−Pt−C$_1$−C$_2$ ≅ 135°). The lowest point on the curve corresponds to R-A1 (H−Pt−C$_1$−C$_2$ = 0°), whereas R-B6 is found at a H−Pt−C$_1$−C$_2$ angle of about 180°. The curve of Figure 2 suggests that besides R-A1 and R-B6 additional minima exist around the angles of 270° and 80°. Therefore full minimizations of these structures were performed, leading to R-C and R-D, respectively, which are shown in Scheme 3.

In contrast to the R-A1 and R-B6 forms, the olefin in these structures is oriented in a plane more or less perpendicular to the plane formed by Pt, P$_1$, and P$_2$. It is seen from Table 2 that, at the HF level, R-C and R-D are even more stable than R-B6. However, at all other levels of theory, the "in-plane" forms are consistently favored over both R-C and R-D. Figure 2 clearly shows that rotation from R-A1 to R-B6 via R-C, or, in terms of the H−Pt−C$_1$−C$_2$ angle, from 0° over 270° to 180°, is the most favorable. This is due, of course, to the fact that in such a transformation the methyl group of propene is not passing under the P$_2$-phosphine. A barrier of 10 kJ/mol results for this rotation. Both the latter energy barrier at 315° and the one at 135° have been recalculated at the other levels of theory, and the results are shown in Table 2. It turns out that the highest energy barrier for rotation amounts to 19.1 kJ/mol at the B3PW91 level of theory and 20.0 and 20.2 kJ/mol for MP2//HF and MP2//B3PW91, respectively. The lowest energy path from R-A1 to R-B6, however, passes an energy barrier of only 13.0 kJ/mol at the B3PW91 level and 16 kJ/mol for both MP2 calculations. In summary, the small energy differences between different coordination modes of the olefin and the low barrier to rotate from R-A1 to R-B6 suggest that both forms can easily interconvert. Although the corresponding rotational energy profiles for PF$_3$- and PMe$_3$-containing complexes have not been calculated, we believe that rotation of the olefin in these systems is also facile, since it is essentially the same process.

Table 7. Optimized Geometrical Parameters of $Pt(PMe_3)_2H^+$ Related Species (Angles in deg, Distances in Å; See Figure 1 for Shorthand Notations of the Structures and Atom Definitions)

PMe_3		Pt−P_1	Pt−P_2	Pt−C_1	Pt−H	C_1−C_2	C_2−H	P_1−Pt−P_2	P_1−Pt−H	P_2−Pt−C_1	H−Pt−C_1−C_2
R-A2	HF	2.332	2.480	2.338	1.575	1.360	2.270	101.6	79.1	84.5	10.2
	B3PW91	2.315	2.411	2.233	1.593	1.391	2.146	101.2	77.5	83.7	11.1
R-A3	HF	2.330	2.472	2.338	1.583	1.358	2.292	102.1	75.9	86.8	10.6
	B3PW91	2.317	2.409	2.227	1.599	1.390	2.152	101.7	74.6	86.4	10.5
TS-A5	HF										
	B3PW91	2.327	2.353	2.162	1.633	1.420	1.669	100.4	85.4	92.2	5.1
TS-A3	HF	2.389	2.392	2.150	1.641	1.417	1.593	103.3	85.1	93.9	2.6
	B3PW91										
P-A2	HF	2.442	2.321	2.075	1.832	1.486	1.220	105.0	92.6	94.4	0.9
	B3PW91	2.364	2.284	2.094	1.803	1.479	1.247	105.3	91.9	93.6	1.4
P-A3	HF	2.450	2.320	2.070	1.830	1.483	1.224	103.9	91.9	95.9	0.3
	B3PW91	2.371	2.282	2.090	1.801	1.477	1.252	104.5	90.5	95.6	1.2
R-B5	HF	2.329	2.487	2.438	1.573	1.352	2.338	98.8	77.5	86.6	−25.7
	B3PW91	2.315	2.416	2.297	1.591	1.385	2.185	99.0	75.8	86.3	−22.2
R-B3	HF	2.331	2.488	2.450	1.576	1.351	2.370	101.9	74.7	86.8	−31.2
	B3PW91	2.316	2.413	2.305	1.594	1.384	2.221	101.6	73.3	86.6	−28.7
TS-B5	HF	2.385	2.404	2.190	1.627	1.409	1.604	100.7	86.1	93.9	−5.6
	B3PW91	2.335	2.361	2.202	1.627	1.417	1.662	100.3	83.8	92.5	−7.1
P-B5	HF	2.450	2.319	2.082	1.858	1.492	1.195	102.9	92.5	96.4	−1.9
	B3PW91	2.371	2.282	2.110	1.823	1.484	1.221	102.6	91.1	96.7	−2.5

PMe_3		Pt−P_1	Pt−P_2	Pt−C_1	Pt−C_2	Pt−N	N−C	P_1−Pt−P_2	P_1−Pt−N	P_2−Pt−C_1	P_2−Pt−C_2
P−A2-MeCN	HF	2.493	2.311	2.111		2.148	1.127	100.9	89.0	85.3	
	B3PW91	2.417	2.272	2.121		2.062	1.152	101.2	89.6	85.1	
P−B2-MeCN	HF	2.506	2.315		2.131	2.144	1.127	100.2	88.0		85.0
	B3PW91	2.423	2.274		2.144	2.069	1.153	100.6	88.7		84.4

Table 8. Relative Energies (kJ/mol) of the $Pt(PMe_3)_2H^+$ Related Species (See Figure 1 for the Shorthand Notation of the Structures)

	HF	MP2//HF	B3PW91	MP2//B3PW91
		$Pt(PMe_3)_2H^+$ + Propene Reaction[a]		
R-A2	1.0	0.5	−1.0	−2.0
R-A3	0.0	0.0	0.0	0.0
R-B5	9.3	1.8	4.5	−1.5
R-B3	10.5	5.8	6.8	2.6
TS-A5			2.4	3.6
TS-A3	18.5	−2.4		
TS-B5	31.9	−1.0	11.0	7.1
P-A2	5.2	−7.4	−7.2	1.1
P-A3	7.5	−6.7	−6.0	2.0
P-B5	12.5	−8.5	−5.3	−0.6
		Insertion Barrier/Elimination Barrier		
TS-A5			3.4/9.6	5.6/2.5
TS-A3	18.5/11.0	−2.4/4.3		
TS-B5	22.6/19.4	−2.8/7.5	6.5/16.3	8.6/7.7
		Rotation Barrier P-B1 → P-B1		
0°[b]	26.1	56.5	38.8	53.9
		Products $Pt(PMe_3)_2$(propyl)$(CH_3CN)^+$[c]		
P-A2-MeCN	0.0	0.0	0.0	0.0
P-B2-MeCN	14.0	1.4	8.8	−0.3

[a] Relative energy with respect to R-A3. [b] Relative energy with repsect to P-B1; see text for angle definition. [c] Relative energy with respect to P-A2-MeCN.

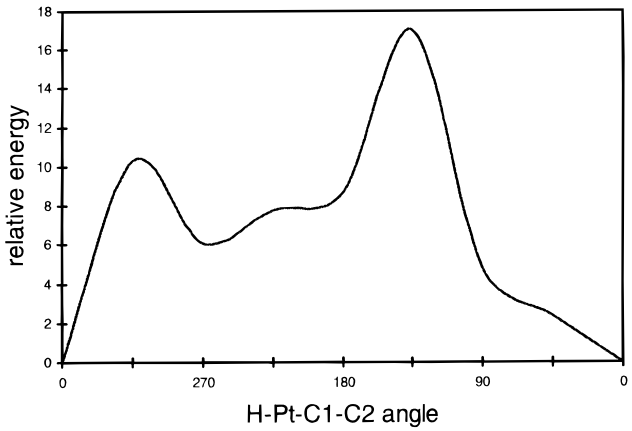

Figure 2. Potential energy profile for variation of the H−Pt−C_1−C_2 angle in $Pt(PH_3)_2(H)$(propene)$^+$ (R-A1), obtained at the HF level.

Scheme 3

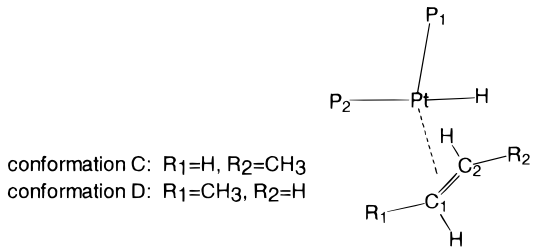

conformation C: R_1=H, R_2=CH_3
conformation D: R_1=CH_3, R_2=H

3.3.2. Rotation around the Pt−C Bond in $Pt(PH_3)_2(Pr)^+$. As seen in a previous section, a β-agostic alkyl complex is formed immediately after the insertion step. The essential step in the double-bond isomerization is then rotation around the C_2−Pt bond, followed by β-elimination to yield the isomerized olefin complex. This rotation was considered for the direct insertion product P-B1, by constraining various H_1−C_2−Pt−P_2 angles and relaxing the other geometrical parameters (see Figure 3 for atom definitions). The resulting energy profile is shown in Figure 3 and is symmetrical around 180°. For clarity, Figure 3 also contains schematic drawings of the different conformations and transformations among them. Two different minima are seen: one at 60° and another at 180°. While the former corresponds to the direct insertion product, P-B1, having β-agostic interaction, no β-agostic interaction is present in the latter. The energy profile also shows two different barriers, one at 0° and one at 150°. Similar to the olefin rotation discussed above, the first barrier corresponds to a rotation such that no repulsion with the P_2-phosphine is encountered (path A in Figure 3), whereas the one at 150° (path B in Figure 3) involves repulsion between the methyl group and the P_2-phosphine. On the

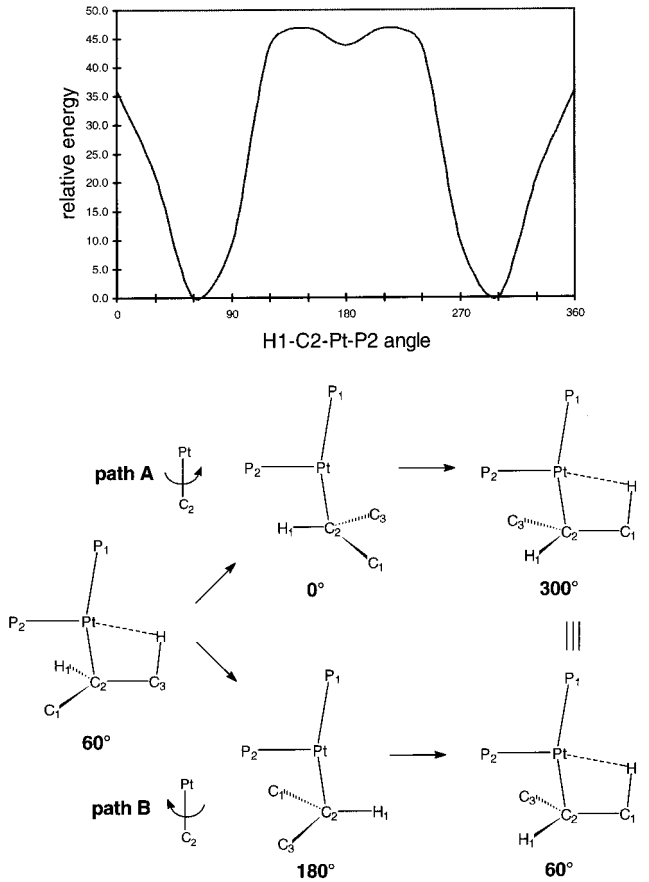

Figure 3. Potential energy profile for rotation around the Pt−C$_2$ bond in P-B1.

Scheme 4

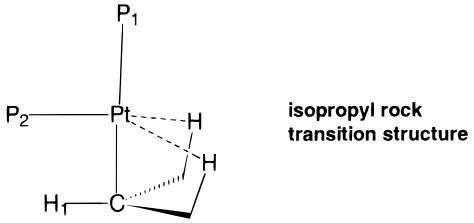

average, the latter barrier is about 13 kJ/mol larger than the former. Obviously, to change from a β-H(C$_3$) to a β-H(C$_1$) interaction in P-B1, the system will proceed via the lowest energy path A. The energy for it ranges from 35.8 kJ/mol (HF) to 67.7 kJ/mol (MP2//HF). As such, this barrier represents the highest one encountered during a complete isomerization cycle, and therefore, we also calculated it for PF$_3$- and PMe$_3$-containing systems. The results are shown in Tables 6 and 8. As can be seen, the barrier slowly decreases in the order PH$_3$ → PF$_3$ → PMe$_3$. For all systems considered, it remains however the rate-determining barrier for isomerization. The transition structure at the H$_1$−C$_2$−Pt−P$_2$ angle of 0° is schematically shown in Scheme 4.

This type of process has in fact been termed an "isopropyl rock" by Green, Bercaw, et al.[38,39] and involves a transition state in which two β-hydrogens simultaneously coordinate to the Pt center. Very recently, the dynamics of the β-agostic isopropyl palladium complex (Ar−N=CR−CR=N−Ar)Pd(*i*-Pr)$^+$ has been studied by variable-temperature ^{1}H and ^{13}C NMR.[40] It was thereby found that the barrier for interchange of the agostic and nonagostic methyl groups amounts to 40 kJ/mol. This barrier is in good agreement with our calculated B3PW91 rotational barriers ranging from 38.8 kJ/mol (PMe$_3$ system) to 47.1 kJ/mol (PH$_3$ system). As such, our calculations provide supplemental evidence for the isopropyl rock as intermediate in methyl group exchange.

3.3.3. Influence of Acetonitrile. As noted in the Introduction, Spencer et al. have demonstrated the ethene-hydride/ethyl equilibrium of a bis-phosphine platinum ethyl complex in diethyl ether as a solvent.[20] These authors also noted that upon addition of acetonitrile, the β-agostic interaction was easily displaced by nucleophilic attack of CH$_3$CN.[20] Therefore, we also considered 4-coordinated alkyl complexes without β-interaction and CH$_3$CN as a fourth ligand. In such a case, double-bond isomerization could take place by association and dissociation of CH$_3$CN, as shown in Scheme 5.

Even though extensive attempts have been made, no transition structure could be located for the association/dissociation of a CH$_3$CN molecule. This observation indicates that the energy barrier for this process is probably very low, which is in line with the findings of Spencer et al.[20] The reaction energy for association of a CH$_3$CN molecule has been calculated for both linear and branched alkyl complexes and for all phosphines under consideration. The results are shown in Table 9. They indicate that the association of acetonitrile is a strongly exothermic process with reaction energies ranging from 85 kJ/mol for Pt(PMe$_3$)$_2$(Pr)$^+$ to 122 kJ/mol for Pt(PF$_3$)$_2$(*i*-Pr)$^+$ (B3PW91 values). While HF is in good agreement with B3PW91, the MP2 method predicts reaction energies being about 10 kJ/mol larger. Thus, dissociation of CH$_3$CN, which is then the crucial step in isomerization, seems to be a rather difficult process. Note, however, that the reaction energy calculated in this way in fact represents the gas-phase dissociation energy. Since we deal with charged particles on one hand (Pt(PR$_3$)$_2$(Pr)$^+$, Pt(PR$_3$)$_2$(Pr)(CH$_3$CN)$^+$) and an electron-rich molecule on the other hand (CH$_3$CN), it can be expected that this dissociation energy is considerably different when calculated in a surrounding solvent. Therefore, Table 9 also includes single-point energy calculations at the HF and B3PW91 levels with the SCI−PCM method for estimating solvation effects. In these calculations, ϵ has been taken to be 39.5, the dielectric constant of acetonitrile. It turns out then that the reaction energies are considerably reduced by about 20−30 kJ/mol. However, the dissociation of CH$_3$CN still remains a rather difficult process, and thus it could be argued that, once coordinated, acetonitrile is not likely to dissociate at all. We therefore tried to calculate 5-coordinated olefin complexes and a transition state, as shown in Scheme 6.

Although various attempts to locate such 5-coordinated transition structures or π-complexes were made, dissociation of either the olefin or a phosphine ligand was seen. This observation seems to be in contrast with recent calculations of Rocha and Almeida, who located

(38) Green, M. L. H.; Sella, A.; Wong, L.-L. *Organometallics* **1992**, *11*, 2650.

(39) Bercaw, J. E.; Burger, B. J.; Green, M. L. H.; Santarsiero, B. D.; Sella, A.; Trimmer, M. S.; Wong, L.-L. *J. Chem. Soc., Chem. Commun.* **1989**, 734.

(40) Tempel, D. J.; Brookhart, M. *Organometallics* **1998**, *17*, 2290.

Scheme 5

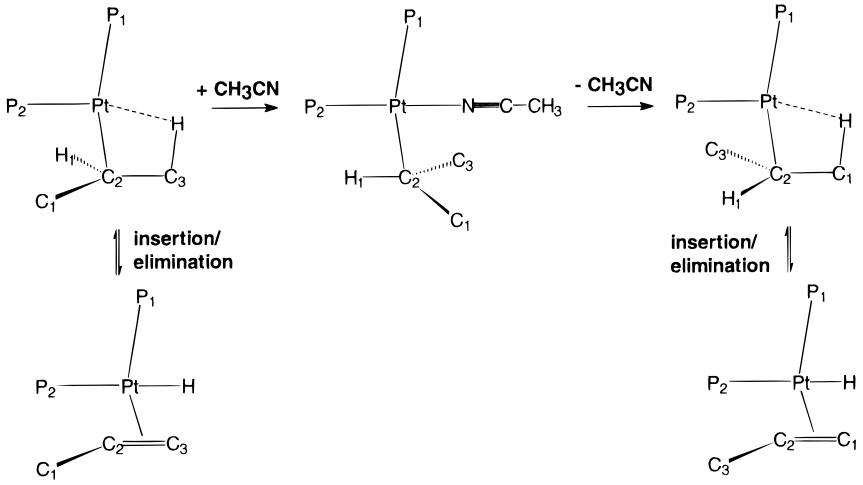

Table 9. Reaction Energies at Various Levels of Theory

	HF	MP2// HF	B3PW91	MP2// B3PW91	SCI-PCM HF	SCI-PCM B3PW91
Displacement of the β-Agostic Interaction by MeCN						
$Pt(PH_3)_2(Pr)^+ + MeCN \rightarrow Pt(PH_3)_2(Pr)MeCN^+$	−105.5	−117.1	−104.3	−120.0		
$Pt(PH_3)_2(i\text{-}Pr)^+ + MeCN \rightarrow Pt(PH_3)_2(i\text{-}Pr)MeCN^+$	−99.7	−118.9	−99.4	−115.6	−80.0	−71.3
$Pt(PF_3)_2(Pr)^+ + MeCN \rightarrow Pt(PF_3)_2(Pr)MeCN^+$	−124.8	−136.0	−122.1	−138.4		
$Pt(PF_3)_2(i\text{-}Pr)^+ + MeCN \rightarrow Pt(PF_3)_2(i\text{-}Pr)MeCN^+$	−118.8	−136.2	−116.2	−139.3	−77.8	−82.2
$Pt(PMe_3)_2(Pr)^+ + MeCN \rightarrow Pt(PMe_3)_2(Pr)MeCN^+$	−87.0	−104.7	−84.7	−107.6		
$Pt(PMe_3)_2(i\text{-}Pr)^+ + MeCN \rightarrow Pt(PMe_3)_2(i\text{-}Pr)MeCN^+$	−80.2	−102.3	−77.8	−106.1	−80.3	−59.6
Phosphine Displacement Reactions						
$Pt(PH_3)_2(Pr)MeCN^+ + 2\ PF_3 \rightarrow Pt(PF_3)_2(Pr)MeCN^+ + 2\ PH_3$	120.0	81.6	79.1	81.4		
$Pt(PH_3)_2(Pr)MeCN^+ + 2\ PMe_3 \rightarrow Pt(PMe_3)_2(Pr)MeCN^+ + 2\ PH_3$	−98.8	−152.1	−108.9	−154.6		
$Pt(PH_3)_2(i\text{-}Pr)MeCN^+ + 2\ PF_3 \rightarrow Pt(PF_3)2(i\text{-}Pr)MeCN^+ + 2\ PH_3$	118.4	80.2	76.8	79.5		
$Pt(PH_3)_2(i\text{-}Pr)MeCN^+ + 2\ PMe_3 \rightarrow Pt(PMe_3)_2(i\text{-}Pr)MeCN^+ + 2\ PH_3$	−95.1	−148.9	−105.0	−152.8		
$Pt(PH_3)_2(i\text{-}Pr)MeCN^+ \rightarrow Pt(PH_3)_2(H)MeCN^+ + propene$	34.1	102.7	72.8	105.5		
$Pt(PH_3)H(propene)^+ + MeCN \rightarrow Pt(PH_3)_2HMeCN^+ + propene$	−46.1	−17.4	−24.8	−8.4		

Scheme 6

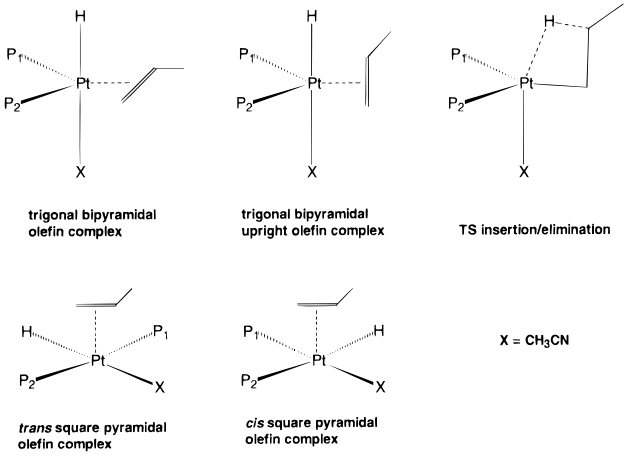

the related $Pt(PH_3)_2(Cl)(H)$(ethene) 5-coordinated π-complexes and transition states.[26] Therefore, we recalculated the 5-coordinated $Pt(PH_3)_2(Cl)(H)$(ethene) at the HF level and the basis set specified in section 2, which indeed yielded stable π-complexes. An attempt to optimize the $Pt(PH_3)_2(Cl)(H)$(propene) molecule, however, resulted in dissociation of the olefin. The existence of 5-coordinated intermediates therefore seems to depend sensitively upon the nature of the olefin.

3.3.4. Conclusion on Double-Bond Isomerization. All things considered, 5-coordinated intermediates are not likely to occur for the processes under investigation in this work. Concerning the 4-coordinated pathways, two different situations appear. (i) In noncoordinating solvents, the isomerization will proceed via the "isopropyl rock" mechanism as outlined above. This mechanism has an energy barrier of 39 kJ/mol for PMe_3 systems, 44 kJ/mol for PF_3 systems, and 47 kJ/mol for PH_3-containing complexes (B3PW91 values). (ii) When coordinating solvent molecules are present, different mechanisms seem possible. On one hand, if the barrier for solvent molecule association is much higher than for an isopropyl rock (e.g., because the approach of the coordinating solvent molecule is sterically hindered), the latter mechanism will be preferred. On the other hand, if solvent molecules coordinate rather easily, isomerization will depend on the dissociation barrier of a solvent molecule. As such, the use of different coordinating solvents should reveal a change in the isomerization rate. In fact, an isomerization experiment using a Pt-phosphine system in CH_3CN solvent at 100 °C is available to us.[41] A first-order kinetics was measured, with a rate constant $k \approx 10^{-2}\ s^{-1}$. Assuming Arrhenius behavior ($\ln k = \ln A - E_a/RT$) and a typical A-value of 10^{13} (the order of a vibrational frequency), we find an Arrhenius activation energy of 105 kJ/mol. Since the Arrhenius activation energy is in general slightly higher than the critical energy, our calculated isomerization barriers (critical energies) for the CH_3CN association/dissociation mechanism are in reasonable agreement

(41) Oevering, H.; Baur, H. Unpublished results.

Scheme 7

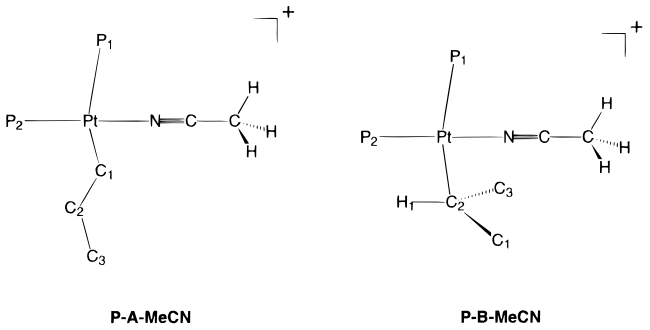

with this crude experimental estimate. Overall, one has to conclude that, in coordinating solvents, both the "isopropyl rock" and solvent association/dissociation mechanisms may be present. It will depend then on the coordination strength of the solvent and the substituents on the phosphines which mechanism is favored.

3.4. Distribution of the Alkyl Products. To our knowledge, only one series of experiments, directly measuring the distribution of different Pt-alkyl complexes, has appeared in the literature.[42,43] It concerns systems of the type (Me$_2$NCS)$_2$Pt(PR$_3$)alkyl, which were heated in xylene solution at 120 °C for a number of days. For R = Me, a mixture of linear and branched propyl complexes was obtained in a 12:1 ratio, in favor of the linear product.[42] The same equilibrium distribution was established starting from either the *n*-propyl or isopropyl complex, which emphasizes the validity of the equilibrium product distribution. This 12:1 ratio corresponds to a free energy difference between both alkyl complexes of 8 kJ/mol. Although these experimentally studied complexes differ considerably from the model systems under investigation in the present work, it is worth comparing our calculated energy differences with this experimental one. Since no β-interaction is present in the (Me$_2$NCS)$_2$Pt(PR$_3$)alkyl complexes, a comparison obviously has to be made with the product complexes containing a solvent molecule. While Tables 2, 6, and 8 contain all relative energies of Pt(PR$_3$)$_2$(Pr/*i*-Pr)(CH$_3$CN)$^+$ systems, their geometrical parameters, which correspond to Scheme 7, can be found in Tables 1, 5, and 7.

Concerning geometry, the Pt−P$_1$ distances tend to be elongated in the MeCN-containing complexes, as compared to the β-agostic product complexes. The trans-effect of the alkyl ligands thus seems somewhat stronger when no β-interaction is present. The Pt−P$_1$ distances also suggest that the isopropyl ligand has a slightly stronger trans-effect than its linear counterpart, which could be due to the difference between a primary and secondary carbon atom. The release of the β-interaction and the accompanying reorientation of the alkyl group upon association of an acetonitrile ligand causes a notable reduction of the P$_2$−Pt−C$_1$ angle by, on the average, 10°. The P$_1$−Pt−P$_2$ angle, for its part, is only slightly reduced.

None of the MP2 calculations yield qualitatively correct relative stabilities, in contrast to HF and B3PW91 calculations, which correctly do so. At the latter level of theory, the linear product for the PH$_3$ system is favored over the branched one by 4.9 kJ/mol. For the PF$_3$ ligands, this gap is reduced to 2.6 kJ/mol, while an enlargement to 8.8 kJ/mol is calculated for PMe$_3$ phosphines. The HF values point toward a similar trend, even though larger energy differences are generally obtained. For the complex containing PMe$_3$ phosphines (which is the best model for the experimental one mentioned above) B3PW91 thus predicts an energy difference of 8.8 kJ/mol in favor of the linear product. This is in fair agreement with the experimental value of 8 kJ/mol.

The effect of different phosphines on the product distributions can be rationalized by considering phosphine displacement reaction energies, which are shown in Table 9. While replacing the parent phosphine with PF$_3$ actually destabilizes the product complexes, substitution of PH$_3$ by PMe$_3$ yields a considerable stabilization. The destabilizing effect of PF$_3$ is larger for the linear product than for the branched one, which explains the reduced energy difference between the PF$_3$-containing alkyl products as compared with the PH$_3$ complexes. An analogous but opposite effect is seen for PMe$_3$ substitution. The reason the stabilizing or destabilizing effects of the phosphines differ for linear and branched products is not yet clear to us.

4. Conclusions

In the present study, a theoretical investigation of the insertion reaction of propene in Pt(PR$_3$)$_2$H$^+$ complexes has been undertaken, for R = H, F, CH$_3$. The calculations indicate that the insertion barriers are generally small. While there is still some significant barrier for R = H of about 10−15 kJ/mol, it is diminished to 3−9 kJ/mol for R = CH$_3$, and almost negligible for R = F (2−4 kJ/mol). The elimination barriers vary from 2 to about 16 kJ/mol, but no clear trends with respect to electron-donating or -withdrawing groups on the phosphines can be seen. The effect of solvent on the insertion/elimination process has not been studied in this work. However, the presence of 5-coordinated intermediates has been shown to be very unlikely, and barriers turn out to be rather small. Therefore, it is temtping to say that solvent molecules will have only a minor effect on the insertion/elimination process.

Insertion of propene can lead to two different alkyl complexes, a linear propyl complex and a branched isopropyl complex. Since the latter can undergo β-elimination in two different ways, double-bond isomerization of propene is possible. This isomerization can proceed via two pathways. If a direct exchange of β-hydrogens occurs in the Pt(PR$_3$)$_2$(*i*-Pr)$^+$ complex by a 60° rotation of the isopropyl ligand (termed the "isopropyl rock" mechanism), a barrier of 38.8 kJ/mol is found for R = CH$_3$, 44.4 kJ/mol for R = F, and 47.1 kJ/mol for R = H (B3PW91 results). These values are in agreement with a recent NMR study indicating a barrier for the isopropyl rock of about 40 kJ/mol. A second isomerization pathway seems possible by association and dissociation of a solvent molecule. Therefore, we studied the energetics for this process, taking CH$_3$CN as a solvent molecule since it is known to displace β-interactions rather easily. Our best estimates of the total energy

(42) Reger, D. L.; Ding, Y.; Garza, D. G.; Lebioda, L. *J. Organomet. Chem.* **1993**, *452*, 263.
(43) Reger, D. L.; Garza, D. G.; Baxter, J. C. *Organometallics* **1990**, *9*, 873.

barrier for this process amount to about 60 kJ/mol for R = CH_3, 71 kJ/mol for R = H, and 82 kJ/mol for R = H. The latter values are also in agreement with a crude estimate of the barrier from kinetic measurements. It is thus seen that, depending on the coordination strength of the solvent and the substituents on the phosphines, there might be a competition between the two mechanisms outlined above. Hence, in noncoordinating solvents, the "isopropyl rock" mechanism is probably the preferred one.

Concerning the distribution of propyl complexes, it turns out that linear complexes are favored over branched ones, in agreement with available experimental data. The energy gap between the two forms decreases in the order R = Me > R = H > R = F. For the latter effect, no satisfying explanation can be found.

In general, HF overestimates all barriers and trends with respect to the B3PW91 level. The MP2 method, on the other hand, is generally in better agreement with the B3PW91 calculations. Whether either the MP2 or the B3PW91 method should be considered to be most reliable is difficult to assess. For relative stabilities, higher level calculations at the QCISD level of theory as well as available experimental data strongly suggest that the B3PW91 method is more reliable than the MP2 method. It has also been shown previously that DFT methods often turn out to be superior to MP2 in treating transtion metal systems.[44,45] Therefore, for the present study, the B3PW91 results should be considered the most useful in drawing conclusions.

OM9806895

(44) Ricca, A.; Bauschlicher, C. W., Jr. *Theor. Chim. Acta* **1995**, *92*, 123.
(45) Stanton, R. V.; Merz, K. M., Jr. *J. Chem. Phys.* **1994**, *100*, 434.